PHYSICAL REVIEW B **87**, 161201(R) (2013)

Defect engineering of $BaSnO_3$ for high-performance transparent conducting oxide applications

David O. Scanlon*

University College London, Kathleen Lonsdale Materials Chemistry, 20 Gordon Street, London WC1H 0AJ, United Kingdom

(Received 19 January 2013; revised manuscript received 10 April 2013; published 22 April 2013)

The high cost and low abundance of indium has driven research to find In-free *n*-type transparent conducting oxides (TCOs). La-doped cubic perovskite $BaSnO_3$ has been reported to possess electron mobilities as high as 320 $cm^2\,V^{-1}\,s^{-1}$ for carrier concentrations of 8×10^{19} cm^{-3}, comparable to the very best TCOs. To date, however, the origins of conductivity in this material have remained unclear. Here we study the defect chemistry of $BaSnO_3$ using a hybrid density functional theory approach, in order to understand how to control the *n*-type conductivity. We show that in undoped samples, native defects cannot cause high levels of *n*-type conductivity; however, adventitious H present in samples can act as shallow donors. By studying the effect of a range of donor dopants, we pinpoint ideal growth conditions and donor dopants for high-performance *n*-type $BaSnO_3$ samples.

DOI: 10.1103/PhysRevB.87.161201 PACS number(s): 71.20.Nr, 71.55.−i

The combination of electrical conductivity and optical transparency in a single material gives transparent conducting oxides (TCOs) an important role in modern optoelectronic applications such as in solar cells, flat panel displays, and smart coatings.[1–3] The current industry standard *n*-type TCO is In_2O_3:Sn (ITO) which demonstrates conductivities of $\sim 10^4$ $S\,cm^{-1}$, while retaining >90% transparency.[3] Typically extrinsic donor doping is necessary for high-performance *n*-type TCO materials, and *p*-type behavior (hole stability) is thermodynamically unfavorable.[4,5] The overwhelming demand for ITO, coupled with the low natural abundance of indium, has made indium an increasingly expensive commodity, which has led to a large research drive to replace ITO as the industry standard *n*-type TCO.[6,7]

Perovskite structured oxides, with the formula ABO_3, are key materials in the field of "oxide electronics," possessing many diverse physical properties including high-transition-temperature superconductivity, optical transparency, ferroelectricity, piezoelectricity, and photocatalytic activity.[8] The emergence of all-perovskite multilayer heterostructures has refocused interest on the development of perovskite materials with improved functionalities.[9,10] Very recently, the transparent perovskite $BaSnO_3$ has been reported to possess electron mobilities comparable with the best TCOs when La doped.[11–13]

Cheong and co-workers synthesized bulk single crystals of La-doped $BaSnO_3$ possessing a Hall mobility of 103 $cm^2\,V^{-1}\,s^{-1}$, with an *n*-type carrier concentration of ~ 8–10×10^{19} cm^{-3}.[11] The lowest resistivity achieved by the authors was $\sim 5.9 \times 10^{-4}\,\Omega\,cm$ (a conductivity of $\sim 1690\,S\,cm^{-1}$) at room temperature, which is higher than the industry standard TCOs.[1] Previous attempts to donor-dope polycrystalline or epitaxially grown $BaSnO_3$ samples with La or Sb had only managed to produce carrier mobilities up to 0.69 $cm^2\,V^{-1}\,s^{-1}$,[14] but these poor results were attributed to grain boundary contributions in the polycrystalline samples.[11]

Kim *et al.* subsequently reported single-crystal La-doped $BaSnO_3$ with a mobility of 320 $cm^2\,V^{-1}\,s^{-1}$ for a carrier concentration of 8×10^{19} cm^{-3}, the highest reported for *any* TCO.[12] The authors also reported a mobility of 70 $cm^2\,V^{-1}\,s^{-1}$ for epitaxial thin films at a doping level of 4.4×10^{20} cm^{-3}. The resistance did not change significantly even after thermal cycles up to 803 K in air, indicating extremely good oxygen stability.[12,13]

In this Rapid Communication, we utilize hybrid density functional theory (DFT) to present the first analysis of the effect of intrinsic and extrinsic defects in $BaSnO_3$. We demonstrate that (i) native defects in the bulk cannot act as a source of shallow donor in this system meaning that undoped samples will be predominately insulating, and (ii) hydrogen impurities and extrinsic donor dopants such as La, Sb, or F will donate electrons to the conduction band, and are the source of the high conductivities reported experimentally. We discuss the doping behavior of $BaSnO_3$ for a range of growth environments, and provide a blueprint for optimum growth conditions for heavily doped samples.

Computational method. All DFT calculations were performed using the VASP code.[15] Interactions between the core and valence electrons were described within the PAW method.[16] The calculations were performed using the PBE[17] exchange-correlation functional augmented with 25% Hartree-Fock exchange, producing the PBE0 functional.[18] PBE0 has been successful in reproducing the structural and band gap data for Sn(IV) containing metal oxide systems.[5,19] A plane wave cutoff of 400 eV and a *k*-point sampling of $6 \times 6 \times 6$ for the 5 atom unit cell of $BaSnO_3$ were used, with the ionic forces converged to less than 0.01 $eV\text{Å}^{-1}$. The optical transition matrix elements, calculated following Fermi's golden rule, were used to construct the imaginary dielectric function and the corresponding optical absorption spectrum.[20] Defects were calculated in a $3 \times 3 \times 3$ (135) atom supercell with a $2 \times 2 \times 2$ Monkhorst-Pack special *k*-point grid, and all calculations were spin polarized.

The formation energy of a defect with charge state q is given by

$$\Delta H_f(D,q) = (E^{D,q} - E^H) + \sum_i n_i(E_i + \mu_i) + q\left(E_{Fermi} + \epsilon^H_{VBM}\right) + E_{align}[q], \quad (1)$$

where E^H is the total energy of the host supercell and $E^{D,q}$ is the total energy of the defect-containing cell. Elemental reference energies E_i were obtained from calculations on the constituent elements in their standard states, e.g., O_2(g), F_2(g),

TABLE I. Table showing geometrical and electronic structure data for $BaSnO_3$ calculated using HSE06 and PBE0, and compared to known experiments. a, $d_{Sn\text{-}O}$, and $d_{Ba\text{-}O}$ are the lattice parameter and cation-anion interatomic distances, measured in Å, E_g^{ind} is the indirect band gap in eV, and E_g^{dir} is the direct band gap in eV.

	HSE06	PBE0	Expt.
a	4.13	4.13	4.12[30]
$d_{Sn\text{-}O}$	2.07	2.07	2.06[30]
$d_{Ba\text{-}O}$	2.92	2.92	2.92[30]
E_g^{ind}	2.49	3.22	~3.12–3.26[25,31]
E_g^{dir}	2.96	3.68	~3.40–3.50[25,31]

H_2(g), Ba(s), Sn(s), La(s), and Sb(s). E_{Fermi} represents the electron chemical potential, which ranges from the valence to conduction band edges. ϵ_{VBM}^{H} is the eigenvalue of the valence band maximum (VBM) of the bulk material. $E_{align}[q]$ is a correction that (i) accounts for the proper alignment of the electrostatic potential between the bulk and the defective supercells and (ii) accounts for the finite-size effects in the calculation of charged impurities, as outlined by Freysoldt *et al.*[21] All charged defects were calculated by adding (subtracting) the correct amount of electrons to (from) the system, with compensation by the jellium background. The dielectric constant used for $BaSnO_3$ was 20.[22] A correction for band filling by defect levels resonant in the conduction band was also included.[23]

Geometry and electronic structure. $BaSnO_3$ crystallizes in the cubic perovskite structure (space group $Pm3m$), in which the Sn sits on the corner of the cube, coordinated to six oxygen in a perfect octahedron, and each oxygen sits in the middle of a cube edge, coordinated to two Sn. Ba occupies the center of the cubic cell. The calculated structural and band gap data for $BaSnO_3$ are shown in Table I. For comparison we compare the PBE0 functional results to the screened exchange functional (HSE06[24]) and to experiment. Both PBE0 and HSE06 reproduce the experimental lattice constants to within ~0.25%. HSE06 underestimates the experimentally measured *indirect allowed*[25] band gap of ~3.2 eV by about 0.7 eV, whereas PBE0 yields band gap data in much closer agreement with experiment. The conduction band minimum (CBM) is situated at the Γ point, with the VBM situated at the R point. The CBM is dominated by Sn 5s character, and the VBM is composed of O 2p states. The conduction band of $BaSnO_3$ is found to be dispersive around the zone center, with an electron effective mass of $0.22m_e$. This value is consistent with the electron effective masses of other high-mobility oxides.[26–29]

To understand the difference between the *fundamental* indirect allowed band gap and the direct allowed *optical* band gap, we have computed the optical absorption spectra for $BaSnO_3$, with the results presented in Fig. 1(b). The onset of optical absorption occurs at 3.68 eV, corresponding to the VB-CB seperation at the Γ point, in good agreement with experimental values.[25,31] Analysis of the symmetry-allowed direct VB-CB transitions confirms that the band gap at the Γ point corresponds to the optical band gap.

Thermodynamic limits. By varying the chemical potentials μ_i, we can simulate the effect of varying the partial pressures

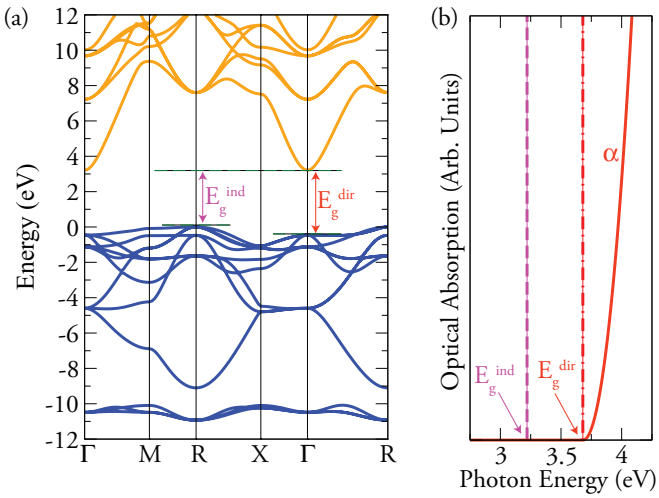

FIG. 1. (Color online) The PBE0 calculated (a) band structure for $BaSnO_3$, and (b) theoretical optical absorption onset of $BaSnO_3$.

experimentally, setting the conditions under which $BaSnO_3$ forms. In this way, we can determine the optimum conditions for n-type defect formation, within the constraint of the calculated enthalpy of the host: $\mu_{Ba} + \mu_{Sn} + 3\mu_O = \Delta H_f^{BaSnO_3}$. To avoid precipitation into solid elemental Ba, Sn, and gaseous O_2 we also require $\mu_{Ba} \leqslant 0, \mu_{Sn} \leqslant 0, \mu_O \leqslant 0$. The chemical potentials are further constrained by the decomposition of $BaSnO_3$ into binary compounds: $\mu_{Sn} + \mu_O \leqslant \Delta H_f^{SnO}$, $\mu_{Sn} + \mu_O \leqslant \Delta H_f^{SnO_2}$, and $\mu_{Ba} + \mu_O \leqslant \Delta H_f^{BaO}$.

The PBE0 calculated accessible range of chemical potentials for $BaSnO_3$ is illustrated in Fig. 2, in a two-dimensional (μ_{Ba}, μ_{Sn}) plane, following the standard approach.[32,33] The vertices of the stability triangle are formed from the host condition ($\mu_{Ba} + \mu_{Sn} + 3\mu_O \leqslant \Delta H_f^{BaSnO_3}$), giving the limits of Ba/Sn rich, Ba-poor, and Sn-poor environments. Taking into account the constraints imposed by the competing binary

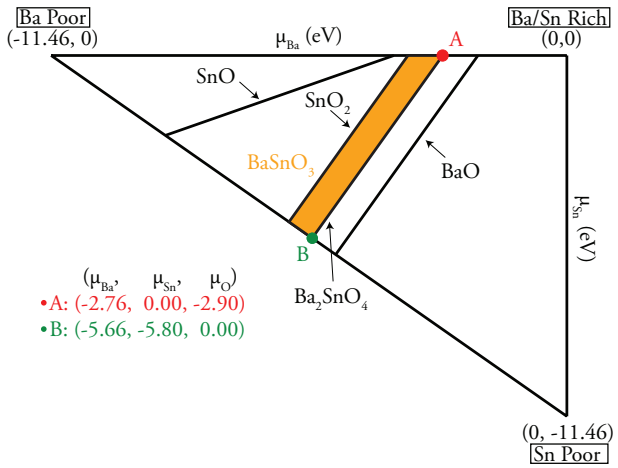

FIG. 2. (Color online) Illustration of the accessible (μ_{Ba}, μ_{Sn}) chemical potential range. The triangle vertices are determined by the formation enthalpy of $BaSnO_3$. Limits imposed by the formation of competing binary and ternary oxides result in the stable region shaded yellow. Environments A, B, C, D are indicated by the red, pink, green, and blue spheres, respectively.

oxides and the ternary Ba_2SnO_4 phase, the stable range of (μ_{Ba}, μ_{Sn}) for $BaSnO_3$ is shaded orange in Fig. 2. Within these boundaries, we explicitly considered two environments (A and B) as indicated in Fig. 2. A corresponds to Sn-rich, Ba-rich, and O-poor conditions, and is expected to be optimum for *n*-type defect formation, whereas B represents the Sn-poor/O-rich limit with Ba also poor, and is expected to favor the formation of *p*-type defects.

Under the different sets of conditions, the solubilities of extrinsic defect-related species are limited by the formation of secondary phases; i.e., $x\mu_M + y\mu_O \leqslant \Delta H_f^{M_xO_y}$. We have therefore calculated the formation energy of La_2O_3, Sb_2O_5, and H_2O using the same calculation parameters as for bulk $BaSnO_3$. In the case of F, which substitutes on the O site, the solubility was determined by the formation of $\Delta H_f^{SnF_4}$.

Defects considered. The native *n*-type defects considered in this study include the oxygen vacancy (V_O), Sn on Ba antisite (Sn_{Ba}), tin interstitial (Sn_i), and barium interstitial (Ba_i), while the *p*-type defects considered were the barium vacancy (V_{Ba}), tin vacancy (V_{Sn}), Ba on Sn antisite (Ba_{Sn}), and oxygen interstitial (O_i). In addition, H was incorporated in a number of lattice positions, namely hydrogen in an oxygen lattice site (H_O) and four different interstitial positions. The interstitial positions tested were the perfect interstitial site, two anion antibonding sites 1 Å from a lattice oxygen (one pointing towards a neighboring O atom, H_i^{AB1}, and one pointing towards a neighboring Ba, H_i^{AB2}), and one bond centered hydrogen, in the direction of the O-Sn bond (H_i^{BC}), as illustrated in Fig. 3. As plausible *n*-type dopants, we have selected La and Sb as these have been routinely utilized as dopants in $BaSnO_3$, as well as previously untested F doping. Fluorine has long been known to be an excellent *n*-type dopant in SnO_2.[34] La and Sb dopants have been considered on the Sn site (X_{Sn}) and the Ba site (X_{Ba}), while F doping has been considered on the oxygen site (F_O) and as an interstitial (F_i).

Intrinsic defects. Figures 4(a) and 4(b) show a plot of formation energy as a function of Fermi level for all intrinsic defects under our two chosen chemical potential environments. Under condition A, V_O is the lowest energy intrinsic donor, but is a negative-*U* defect, with the 2+/O transition level 0.37 eV below the CBM. It should be noted that this behavior is consistent with that of V_O in other wide band gap *n*-type TCOs, i.e., ZnO,[23,35–37] SnO_2,[38] Ga_2O_3,[39] and In_2O_3.[40,41] In all these cases, however, the 2+/0 transition level for the V_O is farther from the CBM than in the case of $BaSnO_2$; however, at 0.37 eV below the CBM V_O in $BaSnO_3$ is unlikely to provide high levels of conductivity in this system. Sn_{Ba} is the next most stable defect, and acts as an *ultra*deep donor with +1/0 and +2/+1 transitions levels 0.73 eV and 0.41 eV above the VBM, respectively. It should be noted that although "self-doping" by cation-on-cation antisites can dominate conductivity in other ternary TCOs,[42,43] this is not the case for $BaSnO_3$. The Ba site is $BaSnO_3$ is so large that it can stabilize Sn in the 2+ charge state, and this is the origin of its deep donor nature. Sn_i and Ba_i both act as shallow donors, but are considerably higher in energy and are unlikely to play a large role in conductivity in $BaSnO_3$. The lowest energy native acceptor defect is the V_{Ba}, but it is too high in energy to compensate the V_O and the Sn_{Ba}.

Under oxygen-rich conditions (condition B), the native acceptor defects are much lower in energy and can compensate the native donors. The lowest energy acceptor defect is the oxygen interstitial; however, it relaxes from the ideal interstitial site towards a lattice oxygen, displacing it to form a peroxide (O-O dumbell-like) species, which we will now denote as O_{per}. An O_i on the perfect interstitial site is seen to be quite metastable relative to the O_{per}. This type of behavior has also been noted previously for other wide band gap oxides.[26,29,44,45] Although the formation energy of O_i^{per} at ~2.40 eV under typical *p*-type conditions is much lower than that of the neutral formation energies of V_{Ba}, V_{Sn}, and Ba_{Sn}, its ionization levels are deep in the conduction band, indicating that it will not act as an effective charge compensating defect in $BaSnO_3$. V_{Ba}, V_{Sn}, and Ba_{Sn} are all deep acceptors, with V_{Ba} clearly the dominant acceptor defect for all growth conditions. Under metal-poor/O-rich conditions, the Fermi level will be trapped in the band gap, at the intersection of the V_O^{+2} and the V_{Ba}^{-2}. Therefore, under typical *p*-type conditions, $BaSnO_3$ will be an insulator, with *n*-type conductivity completely compensated. It also indicates that $BaSnO_3$ cannot be made *p* type by intrinsic defects under any conditions.

Extrinsic impurities. In Figs. 4(c) and 4(d) we present a plot of formation energy as a function of Fermi level for our chosen extrinsic defects in $BaSnO_3$ under our two chosen chemical potential environments. Under metal-poor/oxygen-rich conditions [Figs. 4(c)] we can see that the formation energies of H_O, H_i^{AB1}, and H_i^{AB2} are very low, with all three acting as shallow donors in $BaSnO_3$. This is consistent with the reported shallow donor behavior of H in many wide band gap oxides.[26,46–48] As $BaSnO_3$ has been used as a proton conductor,[49] H is very mobile in $BaSnO_3$, with experimentally measured activation energies of proton conduction of 0.35–0.40 eV.[50] La_{Ba}, Sb_{Sn}, and F_O are all shallow donors in this system, with F_O the most soluble defect, followed by La_{Ba} and then Sb_{Sn}. The 0/+1 ionization level for Sb_{Sn} is just below the CBM, whereas the 0/+1 ionization levels for La_{Ba} and F_O are inside the CBM, which explains why La doping has been more successful at creating high-performance $BaSnO_3$ samples.[11–13] Sb_{Ba} is much higher in energy and will not play a role in determining

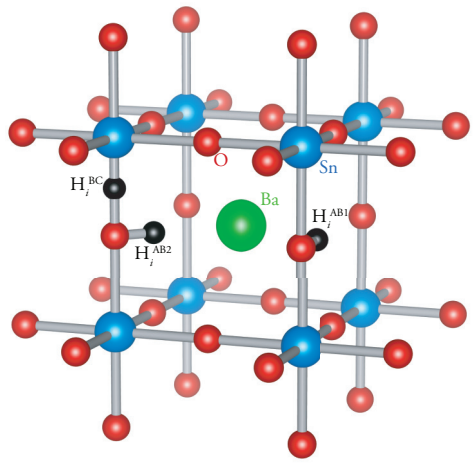

FIG. 3. (Color online) The geometry of H impurities in $BaSnO_3$. The Ba, Sn, O, and H atoms are represented by green, blue, red, and black spheres, respectively.

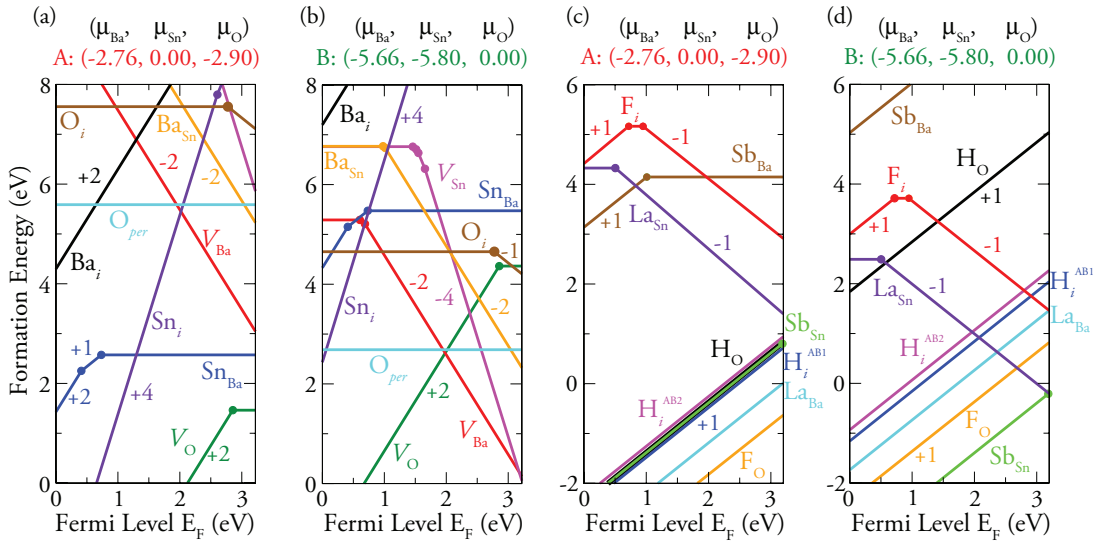

FIG. 4. (Color online) Formation energies for intrinsic defects [(a) and (b)] and extrinsic defects [(c) and (d)] in $BaSnO_3$ under the conditions chosen in Fig. 2. The slope of the lines denotes the charge state; the larger the slope, the bigger the charge state. The solid dots represent the transition levels $\epsilon(q/q')$.

conductivity in $BaSnO_3$ under O-poor conditions. It is a deep *single electron* donor, as once again the large Ba site stabilizes Sb in the +3 oxidation state. La_{Sn} has a formation energy of 4.32 eV and is a deep acceptor, but will not compensate La_{Ba} under these growth conditions. F_i is an amphoteric defect but is too high in energy to compensate the low-energy F_O, which indicates that F doping is a very viable alternative dopant to La for producing a high-performance *n*-type TCO. Hydrogen doping could also be used as a means to adjust the carrier density as it is in other TCOs.[51]

Under O-rich/metal-poor growth conditions [Fig. 4(d)], the formation energy of the H_O, F_O, H_i, and La_{Ba} are increased, as they are all strongly dependent on μ_O. The only shallow donor that becomes more stable under O-rich conditions is Sb_{Sn}, a trend that has also been reported for Sb-doped SnO_2.[52] Under metal-poor conditions, however, it must be noted that the native acceptor defects will be dominant at the CBM, and so at the O-rich/metal-poor limit *n*-type conductivity could be compensated. Indeed we can clearly see that La_{Sn} will compensate La_{Ba} under these conditions. Thus to counteract the effect of compensation by native acceptors and La_{Sn}, care should be taken to produce La-doped samples grown at conditions that are not very metal-poor or very O-rich. F doping is not self-compensated by F_i formation under O-rich conditions, but will be compensated by native defect formation under metal-poor conditions.

Summary. We have demonstrated that none of the native impurities in $BaSnO_3$ can act as shallow defects, and that under O-rich conditions native *n*-type defects will be completely compensated by acceptor defects. Only the introduction of an extrinsic donor impurity can transform $BaSnO_3$ into a degenerate TCO, consistent with experimental reports.[11,12] Adventitious hydrogen is shown to be a shallow donor when incorporated as interstitials and on the O site. We identify F doping as an excellent alternative donor dopant for high-performance TCO applications, and suggest that growth conditions which are not fully O-rich are necessary to limit-self compensation in this system. It is expected that these results will serve as a guide to experimentalists attempting to optimize $BaSnO_3$ and related perovskites for high-performance TCO applications.

Acknowledgments. D.O.S. is grateful to the Ramsay Memorial Trust and University College London for the provision of a Ramsay Fellowship. The work presented here made use of the UCL Legion HPC Facility, the IRIDIS cluster provided by the EPSRC funded Centre for Innovation (EP/K000144/1 and EP/K000136/1), and the HECToR supercomputer through membership of the UK's HPC Materials Chemistry Consortium, which is funded by EPSRC Grant No. EP/F067496.

*d.scanlon@ucl.ac.uk

[1]G. Thomas, Nature (London) **389**, 907 (1997).

[2]K. Hayashi, S. Matsuishi, T. Kamiya, M. Hirano, and H. Hosono, Nature (London) **419**, 462 (2002).

[3]T. Minami, Semicond. Sci. Technol. **20**, S35 (2005).

[4]C. R. A. Catlow, A. A. Sokol, and A. Walsh, Chem. Commun. **47**, 3386 (2011).

[5]D. O. Scanlon and G. W. Watson, J. Mater. Chem. **22**, 25236 (2012).

[6]L. Wang, D. W. Matson, E. Polikarpov, J. S. Swensen, C. C. Bonham, L. Cosimbescu, J. J. Berry, D. S. Ginley, D. J. Gaspar, and A. B. Padmaperuma, J. Appl. Phys. **107**, 043103 (2010).

[7]A. Walsh, A. B. Kehoe, D. J. Temple, G. W. Watson, and D. O. Scanlon, Chem. Commun. **49**, 448 (2013).

[8]T. Wolfram and S. Elliatioglu, *Electronic and Optical Properties of d-Band Perovskites* (Cambridge University Press, New York, 2006).

[9]W. Meevasana, P. D. C. King, R. H. He, S. K. Mo, M. Hashimoto, A. Tamai, P. Songsiriritthigul, and Z. X. Baumberger, Nat. Mater. **10**, 114 (2011).
[10]P. D. C. King, R. H. He, T. Eknapakul, P. Buaphet, S. K. Mo, Y. Kaneko, S. Harashima, Y. Hikita, M. S. Bahramy, C. Bell *et al.*, Phys. Rev. Lett. **108**, 117602 (2012).
[11]X. Luo, Y. S. Oh, A. Sirenko, P. Gao, T. A. Tyson, K. Char, and S. W. Cheong, Appl. Phys. Lett. **100**, 172112 (2012).
[12]H. J. Kim, U. Kim, H. M. Kim, T. H. Kim, H. S. Mun, B. G. Jeon, K. T. Hong, W. J. Lee, C. Ju, K. H. Kim *et al.*, Appl. Phys. Exp. **5**, 061102 (2012).
[13]H. J. Kim, U. Kim, T. H. Kim, J. Kim, H. M. Kim, B. G. Jeon, W. J. Lee, H. S. Mun, K. T. Hong, J. Yu, K. Char, and K. H. Kim, Phys. Rev. B **86**, 165205 (2012).
[14]H. F. Wang, Q. Z. Liu, F. Chen, G. Y. Gao, W. B. Wu, and X. H. Chen, J. Appl. Phys. **101**, 106105 (2007).
[15]G. Kresse and J. Furthmüller, Phys. Rev. B **54**, 11169 (1996).
[16]G. Kresse and D. Joubert, Phys. Rev. B **59**, 1758 (1999).
[17]J. P. Perdew, K. Burke, and M. Ernzerhof, Phys. Rev. Lett. **77**, 3865 (1996).
[18]C. Adamo and V. Barone, J. Chem. Phys. **110**, 6158 (1999).
[19]P. Agoston, C. Korber, A. Klein, M. J. Puska, R. M. Nieminen, and K. Albe, J. Appl. Phys. **108**, 053511 (2010).
[20]M. Gajdos, K. Hummer, G. Kresse, J. Furthmüller, and F. Bechstedt, Phys. Rev. B **73**, 045112 (2006).
[21]C. Freysoldt, J. Neugebauer, and C. G. Van de Walle, Phys. Rev. Lett. **102**, 016402 (2009).
[22]P. Singh, B. J. Brandenburg, C. P. Sebastian, P. Singh, S. Singh, D. Kumar, and O. Parkash, Jpn. J. Appl. Phys. **47**, 3540 (2008).
[23]S. Lany and A. Zunger, Phys. Rev. B **78**, 235104 (2008).
[24]A. V. Krukau, O. A. Vydrov, A. F. Izmaylov, and G. E. Scuseria, J. Chem. Phys. **125**, 224106 (2006).
[25]W. Zhang, J. Tang, and J. Ye, J. Mater. Res. **22**, 1859 (2007).
[26]M. Burbano, D. O. Scanlon, and G. W. Watson, J. Am. Chem. Soc. **133**, 15065 (2011).
[27]A. Walsh, J. L. F. Da Silva, S. H. Wei, C. Korber, A. Klein, L. F. J. Piper, A. DeMasi, K. E. Smith, G. Panaccione, P. Torelli *et al.*, Phys. Rev. Lett. **100**, 167402 (2008).
[28]A. B. Kehoe, D. O. Scanlon, and G. W. Watson, Phys. Rev. B **83**, 233202 (2011).
[29]D. O. Scanlon, A. B. Kehoe, G. W. Watson, M. O. Jones, W. I. F. David, D. J. Payne, R. G. Egdell, P. P. Edwards, and A. Walsh, Phys. Rev. Lett. **107**, 246402 (2011).
[30]Y. Hinatsu, J. Solid State Chem. **122**, 384 (1996).
[31]H. Mizoguchi, H. W. Eng, and P. M. Woodward, Inorg. Chem. **43**, 1667 (2004).
[32]C. Persson, Y.-J. Zhao, S. Lany, and A. Zunger, Phys. Rev. B **72**, 035211 (2005).
[33]D. O. Scanlon, P. D. C. King, R. P. Singh, A. de la Torre, S. McKeown Walker, G. Balakrishnan, F. Baumberger, and C. R. A. Catlow, Adv. Mater. **24**, 2154 (2012).
[34]Z. Hu, J. Zhang, Z. Hao, Q. Hao, X. Geng, and Y. Zhao, Appl. Phys. Lett. **98**, 123302 (2011).
[35]A. Janotti and C. G. Van de Walle, Appl. Phys. Lett. **87**, 122102 (2005).
[36]F. Oba, A. Togo, I. Tanaka, J. Paier, and G. Kresse, Phys. Rev. B **77**, 245202 (2008).
[37]S. Lany and A. Zunger, Phys. Rev. B **81**, 205209 (2010).
[38]A. K. Singh, A. Janotti, M. Scheffler, and C. G. Van de Walle, Phys. Rev. Lett. **101**, 055502 (2008).
[39]J. B. Varley, J. R. Weber, A. Janotti, and C. G. Van de Walle, Appl. Phys. Lett. **97**, 142106 (2010).
[40]P. Agoston, K. Albe, R. M. Nieminen, and M. J. Puska, Phys. Rev. Lett. **103**, 245501 (2009).
[41]S. Limpijumnong, P. Reunchan, A. Janotti, and C. G. Van de Walle, Phys. Rev. B **80**, 193202 (2009).
[42]H. Peng, J. H. Song, E. M. Hopper, Q. Zhu, T. O. Mason, and A. J. Freeman, Chem. Mater. **24**, 106 (2012).
[43]D. O. Scanlon and G. W. Watson, J. Phys. Chem. Lett. **1**, 3195 (2010).
[44]A. A. Sokol, S. A. French, S. T. Bromley, C. R. A. Catlow, H. J. J. van Dam, and P. Sherwood, Farad. Discuss. **134**, 267 (2007).
[45]P. R. L. Keating, D. O. Scanlon, B. J. Morgan, N. M. Galea, and G. W. Watson, J. Phys. Chem. C **116**, 2443 (2012).
[46]P. D. C. King, R. L. Lichti, Y. G. Celebi, M. Gil, R. C. Vilao, H. V. Alberto, Piroto Duarte, D. J. Payne, R. G. Egdell, I. McKenzie *et al.*, Phys. Rev. B **80**, 081201(R) (2009).
[47]M. H. Du and D. J. Singh, Phys. Rev. B **79**, 205201 (2009).
[48]C. G. Van de Walle, Phys. Rev. Lett. **85**, 1012 (2000).
[49]L. Buannic, F. Blanc, D. S. Middlemiss, and C. P. Grey, J. Am. Chem. Soc. **134**, 14483 (2012).
[50]Y. Wang, Y. Chesnaud, E. Bevillon, and G. Dezanneau, Solid State Ionics **214**, 45 (2012).
[51]A. Kronenberger, A. Polity, D. M. Hofmann, B. K. Meyer, A. Schleife, and F. Bechstedt, Phys. Rev. B **86**, 115334 (2012).
[52]J. B. Varley, A. Janotti, and C. G. Van de Walle, Phys. Rev. B **81**, 245216 (2010).